NJC

Accepted Manuscript

This article can be cited before page numbers have been issued, to do this please use: M. Remelli, D. Bellotti, D. Loboda and M. Rowinska-Zyrek, *New J. Chem.*, 2018, DOI: 10.1039/C8NJ00533H.

ROYAL SOCIETY OF CHEMISTRY

rsc.li/njc

View Article Online
DOI: 10.1039/C8NJ00533H

New Journal of Chemistry

PAPER

Investigation on the metal binding sites of a putative Zn(II) transporter in opportunistic yeast species *Candida albicans*

Received 00th January 20xx,
Accepted 00th January 20xx

DOI: 10.1039/x0xx00000x

www.rsc.org/

Denise Bellotti,[a] Dorota Łoboda,[b] Magdalena Rowińska-Żyrek,[b,*] Maurizio Remelli[a,*]

In the present work, we focus on C4YJH2, a protein sequence of 199 amino acid residues, found in the genome of *Candida albicans*, and suggested to be involved in metal transport. *Candida albicans* is a member of the normal human microbiome; under certain circumstances that allow it to grow out of control, it can transform into a very dangerous fungal pathogen. The most probable Zn(II) binding domain of this sequence was identified at its C-terminus, a histidine-rich region, well conserved in numerous fungal Zn(II) transporters. The Zn(II) binding behaviour towards the three peptides Ac-FHEHGHSHSHGSGGGGGG-NH_2 (residues 131-148), Ac-SHSHSHSHS-NH_2 (residues 157-165), and Ac-FHEHGHSHSHGSGGGGGGSDHSGDSKSHSHSHSHS-NH_2 (residues 131-165) was explored by means of different thermodynamic and spectroscopic techniques. Cu(II) was also investigated since this endogenous metal can compete with Zn(II) for the same binding sites.

The results indicate that the peptides under investigation have the ability to tightly coordinate Zn(II), at physiological pH, thus suggesting that the whole protein sequence can play a role in Zn(II) acquisition and regulation. Cu(II) is able to form even stronger complexes than Zn(II) but it is normally present in very low concentration in the biological environment. The competition between Zn(II) and Cu(II) could be exploited to impair the Zn(II) acquisition routes of *Candida albicans.* Among the two binding sites, the affinity of both Zn(II) and Cu(II) is higher for that located at the residues 131-148, although the coordination geometry is rather different for the two metal ions.

Introduction

Candida albicans is a commensal part of the physiological flora in the oral cavity, skin, gastrointestinal and urogenital tracts. In the case of its pathological overgrowth, it is also the most common fungal pathogen found in humans, the cause of candidiasis, a condition that encompasses infections that range from superficial (such as oral thrush or vaginitis), chronic (reoccurring ulcers or painful sores that require long-term treatment) to systemic and potentially life-threatening candidemia (invasive candidiasis). The condition is usually confined to severely immunocompromised patients (undergoing organ transplantation, major surgery and those with AIDS or neoplastic disease).[1] However, untreated invasive candidiasis is a serious problem also in non-immunosuppressed patients,[2-4] and may ultimately become a greater problem than drug resistant bacterial "superbugs".[5]

Despite the progress of antifungal therapies and the ongoing search for new therapeutic strategies, there is currently only a limited number of truly effective treatments: the ability of pathogenic microorganisms to adapt and therefore resist drug action still causes thousands of deaths every year. One of the biggest obstacles in finding fungus-specific therapeutics is the fact that humans and fungi share essential metabolic pathways (they are both eukaryotes, unlike disease-causing bacteria). Lack of specificity is an important concern in the development of novel, specific agents towards which fungi will not be resistant to. In order to design new antifungal drugs, it is crucial to find and aim at differences in the human and fungal metabolism. One of these differences is the metal transport mechanism and, in particular, the transport of Zn(II) into the fungal cell. Understanding the bioinorganic chemistry of this process is therefore of particular interest; in fact, a deep knowledge of the coordination modes and thermodynamics of metal-metal transporter interactions is the first step towards the design of a highly specific therapeutic.[6-9]

Zn(II) is crucial for the virulence and survival of fungal pathogens in humans, being indispensable, together with Cu(II), in the expression of many metal-proteins and enzymes.[10, 11] Zn(II) uptake is a challenge for microbes, since the concentration of this metal in a free, non-protein bound form, is as low as sub-nanomolar.[12] Cu(II) is not only an endogenous metal which can generally compete with Zn(II) for

[a] *Department of Chemical and Pharmaceutical Sciences, University of Ferrara, via Luigi Borsari 46, I-44121 Ferrara, Italy. E-mail: rmm@unife.it*
[b] *Faculty of Chemistry, University of Wroclaw, F. Joliot-Curie 14, 50-383 Wroclaw, Poland. E-mail: magdalena.rowinska-zyrek@chem.uni.wroc.pl*
[c] **Corresponding authors.*
†Electronic Supplementary Information (ESI) available. See DOI: 10.1039/x0xx00000x

View Article Online
DOI: 10.1039/C8NJ00533H

the same binding sites, but it can take part in the host-microbe "tug of war".[13-15]

C4YJH2 (UniProt Knowledgebase[16]) is a 199 amino acid sequence corresponding to the gene CAWG_03987 found in the strain WO-1 of *Candida albicans*.[17] "CAWG_03987 has domain(s) with predicted cation transmembrane transporter activity, role in transmembrane transport, cation transport and integral to membrane localization".[18] In contrast to most metal-sequestering proteins, C4YJH2 has a significantly higher number of histidine and serine residues, especially in its C-terminal domain, where two sequences containing His alternated with other amino acids are located and can both act as metal binding sites.

In this work, we focus on the interactions of Zn(II) and Cu(II) with three C-terminal C4YJH2 sequences: Ac-FHEHGHSHSHGSGGGGGG-NH_2 (residues 131-148, L1), Ac-SHSHSHSHS-NH_2 (residues 157-165, L2), and Ac-FHEHGHSHSHGSGGGGGGSDHSGDSKSHSHSHSHS-NH_2 (residues 131-165, encompassing the two shorter fragments, L3). The studied sequences are very similar to those present in several putative Zn(II) transporters and proteins involved in metal homeostasis (Scheme S1, ESI†).

Mass spectrometric measurements and potentiometric titrations provided information about stoichiometry, coordination modes and stability of the formed complexes. In combination with spectroscopic techniques, these methods allowed to identify and discuss the metal binding sites of the investigated ligands.

Results and discussion

Ligands protonation

All the peptides L1, L2 and L3 (see Experimental) were protected at their N-terminus by acetylation and at their C-terminus by amidation. The amidic protons of the peptide backbone cannot be spontaneously released in the pH range explored by potentiometry, since they are very weak acids (p*K*a≈15),[19] but they can be displaced by Cu(II) at a suitable pH value, to form complexes. The distribution diagrams for protonation equilibria of L1, L2 and L3 are shown in Figures S1, S2 and S3 (ESI†) and the corresponding constants are reported in Tables S1, S2 and S3 (ESI†). Ligand L1 (Ac-FHEHGHSHSHGSGGGGGG-NH_2) has six groups involved in acid-base reactions: one glutamic acid and five histidines. Glutamic acid has the lowest p*K*a value (4.18), as predictable by its acid moiety; while His residues are characterized by log*K* values ranging from 5.74 to 7.50. Ligand L2 (Ac-SHSHSHSHS-NH_2) contains four basic sites, corresponding to its four histidines. The obtained protonation constants (5.48, 6.08, 6.47, and 7.12) are in excellent agreement with theoretical expectations based on His protonation equilibria.[20] Ligand L3 has fourteen groups involved in acid-base reactions: one glutamic acid, two aspartic acids, ten histidines and one lysine. In the considered pH range 3-9, both the deprotonation of an aspartic acid and the lysine could not be detected. The first two acidic constants of L3, characterized by p*K*a values of 3.52 and 3.90, likely correspond to the second aspartic acid and to the glutamic acid side groups, while the other ten p*K*a values, ranging from 5.14 to 7.78, arise from the deprotonation of the ten histidines. The p*K*a of Lys (necessary for computations but irrelevant on the results in the pH range 3-9) is assumed to be equal to the averaged literature value for Lys-containing peptides, under the same experimental conditions (10.54[21]). Potentiometric data do not allow to understand which specific His residue is involved in each deprotonation step, as all the histidines are almost equivalent from the chemical point of view. For this purpose, NMR studies would be useful and they will be the subject of further investigation.

Zn(II) complexes

All the present results show that L1 and L2 peptides are able to form 1:1 complexes with the Zn(II) ion; no poly-nuclear or bis-complexes have been detected neither by potentiometry nor by mass spectrometry. Formation constant values are shown in Table 1 and the corresponding distribution diagrams are plotted in Fig. 1-3; ESI-MS spectra are instead reported in Fig. S4-S14 (ESI†). Stability constants for the system Zn(II)/L1 have been calculated only up to pH 6, because, at higher pH, precipitation occurred. No precipitation has instead been observed over the explored pH range in the case of L2 and L3.

Zn(II) binds L1 starting from pH 4.3 with the formation of the species $[ZnH_3L]^{4+}$, where the most likely coordination mode is *via* two histidine residues and the carboxyl group of the glutamic acid ($2N_{Im}$; COO^-). The next step involves the release of a third proton with a p*K*a value of 4.9, giving rise to the species $[ZnH_2L]^{3+}$. This complex begins to form at a pH close to that of the previous one. The most likely coordination mode for this species is three histidine residues and one oxygen atom with a tetrahedral geometry, rather common in zinc-transporting proteins.[22-25] Analogously, in the case of L2, the first detected complex $[ZnHL]^{3+}$ is also characterized by the ($3N_{Im}$; O) configuration; in this case, the oxygen atom should belong to a water molecule. Further deprotonation gives rise to the species $[ZnL]^+$ (L1) and $[ZnL]^{2+}$ (L2). In the case of L1, two protons are most likely released almost simultaneously by the remaining two histidines, which are not involved in the coordination. As for L2, the acidic proton of the coordinated water molecule is instead released, giving rise to a ($3N_{Im}$; OH^-) complex. Moreover, at higher pH values, the species $[ZnH_{-1}L]^+$ is formed: the corresponding log*K* value 7.22 is practically identical to that of the fourth His residue (7.12, Table S2, ESI†) which most likely deprotonates without interacting with the metal ion. Further hydrolysis is observed at the most alkaline pH values.

View Article Online
DOI: 10.1039/C8NJ00533H

In the system Zn(II)/L3, the availability of a larger number of histidine residues gives rise to a complicated, pH-dependent, mixture of metal complexes (Fig. 3), where different histidines are coordinated to Zn(II) in a high number of combinations. The MS spectra (Fig. S10-S14, ESI†), recorded at pH 5.30, reveal the presence of both mononuclear ($[ZnH_5L]^{4+}$ at *m/z*=900.6, $([ZnH_4L]\cdot K)^{4+}$ at *m/z*=910.1 and $([ZnH_3L]\cdot K_2)^{4+}$ at *m/z*=919.8) and binuclear ($[Zn_2H_3L]^{4+}$ at *m/z*=916.5) species. The latter complex has been successfully introduced in the speciation model for the fitting of potentiometric data (Table 1). It is reasonable to suppose that, in the complex $[Zn_2H_3L]^{4+}$, the two Zn(II) ions are bound to the two major clusters of histidines, located near the C- and N-terminus, respectively. Thus, the L3 peptide possesses two (most likely) independent coordination sites separated by a rather long linker. It is reasonable to suggest that, in the simultaneous presence of different, competing, metal ions – as it can happen *in vivo* – the two binding sites can be occupied by different metals. This hypothesis could be checked through further thermodynamic studies on the ternary system Cu(II)/Zn(II)/L3, on the basis of the binary speciation models reported here. Circular dichroism measurements performed in the far-ultraviolet spectroscopic range (Fig. S15, ESI†) reveal that there is no significant pH-dependant variation in the secondary structure of Zn(II)/L3 complexes. The band at 200 nm points out the absence of a specific conformation and the prevalence of random coils.

Table 1 Overall stability constants (log *β*) and acid dissociation constants (p*K*a) of zinc(II) complexes with L1, L2 and L3 at *T*=298 K, *I*=0.1 mol dm^{-3} ($NaClO_4$). Values in parentheses are standard deviations on the last significant figure.

Ligand	Species	log *β*	p*K*a
L1	$[ZnH_3L]^{4+}$	24.1 (1)	4.9
	$[ZnH_2L]^{3+}$	19.21 (2)	-
	$[ZnL]^{+}$	7.51 (2)	-
L2	$[ZnHL]^{3+}$	11.55 (3)	5.97
	$[ZnL]^{2+}$	5.58 (2)	7.22
	$[ZnH_{-1}L]^{+}$	-1.65 (4)	8.20
	$[ZnH_{-2}L]$	-9.85 (6)	-
L3	$[ZnH_8L]^{7+}$	62.32 (5)	-
	$[ZnH_6L]^{5+}$	51.65 (6)	-
	$[ZnH_4L]^{3+}$	39.89 (3)	-
	$[ZnH_2L]^{+}$	26.40 (3)	7.84
	$[ZnHL]$	18.57 (7)	8.57
	$[ZnL]^{-}$	10.0 (1)	8.6
	$[ZnH_{-1}L]^{2-}$	1.35 (1)	-
	$[Zn_2H_3L]^{4+}$	38.8 (2)	-

Cu(II) complexes

The three investigated peptides proved to be able to form

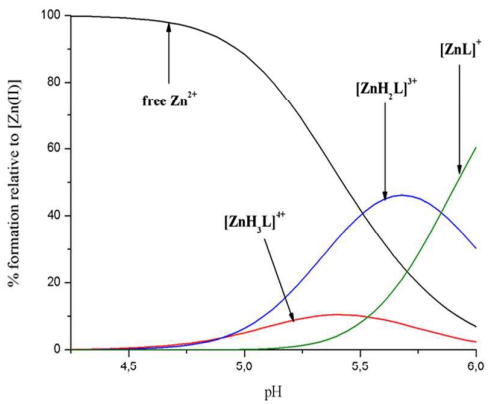

Figure 1 Exemplificative species distribution diagram relative to Zn(II)/L1 complexes; metal/ligand molar ratio = 1 : 1.25.

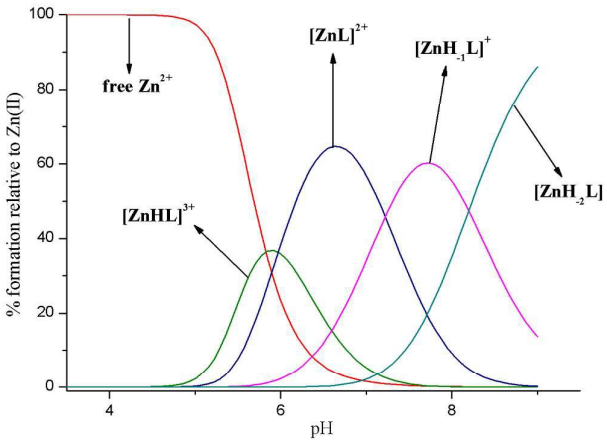

Figure 2 Exemplificative species distribution diagram relative to Zn(II)/L2 complexes; metal/ligand molar ratio = 1 : 1.25.

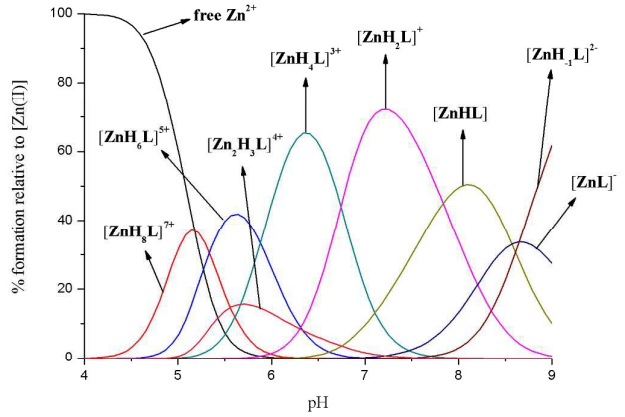

Figure 3 Exemplificative species distribution diagram relative to Zn(II)/L3 complexes; metal/ligand molar ratio = 1 : 1.25.

View Article Online
DOI: 10.1039/C8NJ00533H

stable 1:1 complexes with the Cu(II) ion; no poly-nuclear or bis-complexes have been detected neither by potentiometry nor by mass spectrometry, under the experimental conditions here employed. Complex-formation constants are reported in Table 2 and the corresponding distribution diagrams are plotted in Fig. 4-6; ESI-MS results are instead showed in Fig. S16-S25 (ESI†), UV-Vis spectra in Fig. S26-S28 (ESI†) and CD spectra in Fig. S29-S32 (ESI†).

Cu(II) starts to interact with L1 at pH lower than 3 and the first detected complex is $[CuH_4L]^{5+}$. The stoichiometry of this species indicates that two acid/base sites are deprotonated and it can be suggested that Cu(II) binds a histidine and the carboxylate group of the glutamic acid (N_{Im}; COO^-), in fact, these two residues (p*K*a values: 5.7 and 4.2, respectively) can be deprotonated at a so acidic pH value only if they are bound to the metal ion.

As for L2 peptide, the stoichiometry of the first detected species is $[CuH_2L]^{4+}$: in this case, potentiometric data do not reveal the formation of the $1N_{Im}$ complex. Most likely, the absence of a carboxylate side chain makes the hypothetical species $[CuH_3L]^{5+}$ less stable than the corresponding complex formed by L1. It can be suggested, for the complex $[CuH_2L]^{4+}$, that two imidazole nitrogens are coordinated to Cu(II). The position of the d–d band of UV-Vis spectra at pH 5 (660 nm, see Fig. S27 and Table S4, ESI†) is in good agreement with this hypothesis.

Two different hypotheses are instead possible for the coordination mode of the first identified complex of L3 peptide, $[CuH_{10}L]^{9+}$, where, besides the Asp residues, two additional acid/base side groups of the ligand are deprotonated. It can be suggested that Cu(II) binds a histidine and the carboxylate group of the Glu residue ($1N_{Im}$; COO^-), as in the case of L1, or that the binding occurs *via* two histidine residues ($2N_{Im}$) while the glutamic acid is still protonated. This latter hypothesis is well supported by the Vis absorption data at pH 3 (see Fig. S28 and Table S5, ESI†), that show a λ_{max}= 660 nm, as expected for a complex where Cu(II) is bound to two imidazole nitrogens.[19] Subsequently, the species $[CuH_9L]^{8+}$, characterized by a protonation constant of 4.0 (Table 2), is compatible with the hypothesis of the mere deprotonation of the Glu residue without any relevant change in the complex geometry; in fact, the wavelength of maximum absorption of the d-d band measured at pH 4 is 658 nm, suggesting again a ($2N_{Im}$) coordination.

Increasing the pH value, Cu(II) binds a larger number of nitrogen atoms, as the blue-shift of Vis spectra for the three ligands indicates (Tables S4-S6, ESI†). In the case of L1, the ($2N_{Im}$; COO^-) and ($3N_{Im}$; COO^-) configurations are the most probable for $[CuH_3L]^{4+}$ and $[CuH_2L]^{3+}$, respectively. Starting from pH 4, the complex loses a further proton to form the species $[CuHL]^{2+}$ where Cu(II) should bind a fourth N-imidazole with a p*K*a = 4.92. It is reasonable that this His residue substitutes the carboxylate group in the equatorial plane, moving it to the axial position. The presence of an axial binding group produces a red-shift in the Vis spectra[19] that can explain the fact that the wavelength of maximum absorption at pH 6.3 (593 nm, see Fig. S26 and Tab. S6, ESI†) is slightly higher than

Table 2 Overall stability constants (log *β*) and acid dissociation constants (p*K*a) of copper(II) complexes with L1, L2 and L3 at *T*=298 K, *I*=0.1 mol dm^{-3} ($NaClO_4$). Values in parentheses are standard deviations on the last significant figure.

Ligand	Species	log *β*	p*K*a
L1	$[CuH_4L]^{5+}$	31.63 (5)	4.30
	$[CuH_3L]^{4+}$	27.33 (5)	4.63
	$[CuH_2L]^{3+}$	22.70 (4)	4.92
	$[CuHL]^{2+}$	17.78 (2)	5.77
	$[CuL]^{+}$	12.00 (2)	-
	$[CuH_{-2}L]^{-}$	-3.04 (2)	8.43
	$[CuH_{-3}L]^{2-}$	-11.47 (3)	-
L2	$[CuH_2L]^{4+}$	20.00 (2)	-
	$[CuL]^{2+}$	10.04 (2)	-
	$[CuH_{-2}L]$	-4.50 (2)	8.94
	$[CuH_{-3}L]^{-}$	-13.44 (4)	-
L3	$[CuH_{10}L]^{9+}$	73.4 (1)	4.0
	$[CuH_9L]^{8+}$	69.4 (1)	4.1
	$[CuH_8L]^{7+}$	65.30 (8)	4.72
	$[CuH_7L]^{6+}$	60.58 (6)	5.20
	$[CuH_6L]^{5+}$	55.38 (6)	5.72
	$[CuH_5L]^{4+}$	49.65 (7)	6.09
	$[CuH_4L]^{3+}$	43.56 (7)	6.39
	$[CuH_3L]^{2+}$	37.16 (5)	6.83
	$[CuH_2L]^{+}$	30.34 (4)	7.19
	$[CuHL]$	23.14 (2)	-
	$[CuH_{-1}L]^{2-}$	7.01 (2)	-
	$[CuH_{-3}L]^{4-}$	-10,85 (3)	-

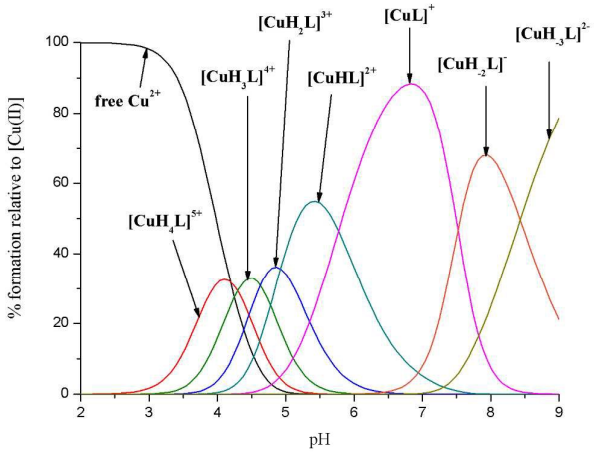

Figure 4 Exemplificative species distribution diagram relative to Cu(II)/L1 complexes; metal/ligand molar ratio = 1:1.25.

View Article Online
DOI: 10.1039/C8NJ00533H

the predicted value for a ($4N_{Im}$) complex (576 nm).[19] At neutral pH, the species $[CuL]^+$ is formed from the deprotonation of a histidine residue not involved in the coordination (d–d band at 590 nm).

A ($4N_{Im}$) configuration is also hypothesized for the $[CuL]^{2+}$ complex formed by the L2 ligand at pH 6. Since the corresponding ($3N_{Im}$) complex was not detected by potentiometry, a cooperative binding effect can be suggested leading to the coordination of the third and the fourth histidine, in a quick sequence. The formation of a 4N species is also confirmed by EPR spectra (Tables S4 and S6, ESI†).[26]

In the case of L3, when increasing the pH value, several species with the same stoichiometry but different donor atom set can form in solution at the same time, giving rise to a complicated mixture, as it happens in the presence of Zn(II). The formation of macrochelates is also possible. At pH 5, where the species $[CuH_7L]^{6+}$ is the most abundant complex in solution, the first amide proton is displaced by the Cu(II) ion. In fact, CD spectra show a negative band at 309 nm (see Fig. S31 and Table S5, ESI†), attributable to the N-amide charge transfer to the metal ion.[19] The d-d band of Vis spectra is located at 602 nm (pH 5.06) and it is compatible with the hypothesis of a ($2N_{Im}$; N^-) complex.[19] At physiological pH, a mixture of ($2N_{Im}$; N^-) and ($3N_{Im}$; N^-) species can be suggested.

Under alkaline conditions, the remarkable change in the visible CD spectra of Cu(II) complexes with all the three ligands (see Fig. S29-S31, ESI†) suggests an important variation in coordination modes: up to three deprotonated amides of the peptide backbone can gradually substitute imidazole nitrogens in the metal coordination sphere with a square-planar molecular geometry, to form ($2N_{Im}$; $2N^-$) and (N_{Im}; $3N^-$) complexes. The formation of some of these mononuclear Cu(II) complexes has been also confirmed by mass spectrometry (Fig. S16-S25, ESI†)

As a final point, it is worth of note that the experimental far UV-CD spectra for the system Cu(II)/L3 (Fig. S32, ESI†) show the absence of any pH-dependant variation in the secondary structure and the prevalence of random coil conformation (band at 200 nm).

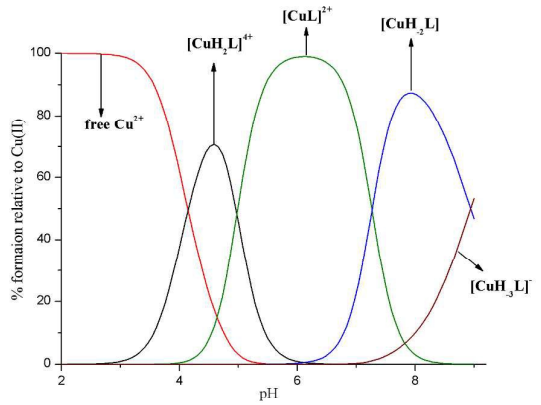

Figure 5 Exemplificative species distribution diagram relative to Cu(II)/L2 complexes; metal/ligand molar ratio = 1:1.25.

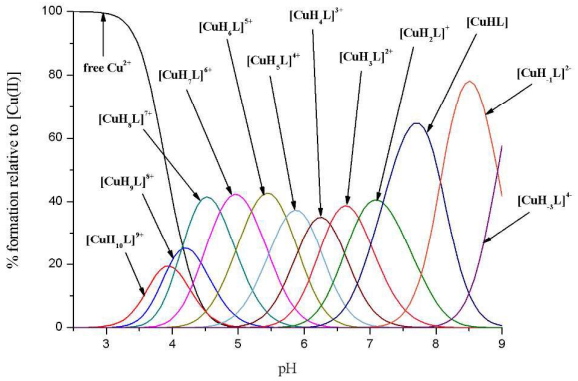

Figure 6 Exemplificative species distribution diagram relative to Cu(II)/L3 complexes; metal/ligand molar ratio = 1:1.25.

A comparison about metal binding abilities

In order to better understand the binding ability of the investigated ligands towards Zn(II) and Cu(II) ions, some competition plots (see Experimental) were built up at equimolar concentrations of ligands and metal ions. As shown in Figures 7 and 8, the L3 species formed with both the Zn(II) and Cu(II) ions are the most stable, while complexes with L2 reach the lowest formation percentages. Complexes with the L1 ligand, containing one more histidine than L2, are in an intermediate situation. These results confirm the previous observation that with the increase of the number of histidines, the coordination becomes more effective.[27-30] It is important to emphasize that L3 contains both the other two peptides. No direct evidence on the preferred metal binding site of L3 is available, although the higher affinity of L1 with respect to L2 suggests that the distribution of mono-nuclear species where the metal ion is bound to L3 is unbalanced in favour of the N-terminal binding site.

In the attempt to get more information on the role played by the number and position of His residues on the coordination ability of the ligand, other competition plots have been built up, where the complex-formation behaviour of L1, L2 and L3 is compared to that of other similar peptides. Four other histidine-rich sequences have been taken into account: *(i)* the fragment of the prion protein of zebrafish, Ac-PVHTGHMGHIGHTGHTGHTGSSGHG-NH_2 (zp-PrP63-87), which contains seven separated His residues;[31, 32] *(ii)* the peptides Ac-EDDAHAHAHAHAG-NH_2 and *(iii)* Ac-EDDHAHAHAHAHG-NH_2,[27] shorter analogues of the peptide pHpG-1 ($EDDH_9GVG_{10}$-NH_2) found in the venom of the snake *Atheris squamigera*,[28, 33] which contain four and five alternate His residues, respectively; *(iv)* the peptide Ac-THHHHYHGG-NH_2, corresponding to the 18-26 domain of the Hpn protein from *H. pylori* and containing five His residues, four of which are consecutive.[34]

View Article Online
DOI: 10.1039/C8NJ00533H

The competition plots that compare the zp-PrP63-87 peptide with L3 (Fig. S33 and S34, ESI†) show a similar trend for both Zn(II) and Cu(II) complexes and confirm that the larger the number of histidines in the sequence, the better the ability to bind both Zn(II) and Cu(II) ions.

A comparison between L2 and Ac-EDDAHAHAHAHAG-NH_2 – both containing four histidines but separated by serine or alanine residues, respectively – in the case of the Cu(II) ion, shows a similar trend for both the ligands up to pH about 5 (Fig. S35, ESI†). On the other hand, Cu(II)/L2 complexes are instead significantly more stable at higher pH values, where the Cu(II)-amide binding comes into play. Evidently, the presence of (non-coordinating) serines has an impact on amide deprotonation, possibly through its electronic effect on amidic nitrogens, making amide protons more acidic. In addition, if the EDD- sequence is involved in Cu(II) coordination, this could somehow hinder the binding with amides. On the contrary, Figure S36 (ESI†) shows that the peptide sequence Ac-EDDAHAHAHAHAG-NH_2 is a better ligand for Zn(II) than the serine-substituted sequence L2, even though the difference between the two curves is not excessive (25% at physiological pH). In this case, Zn(II) is not able to deprotonate N-amides, which do not come into play. The coordination mode is almost the same for both the peptides: Zn(II) binds L2 *via* ($3N_{Im}$; H_2O), while Zn(II)/Ac-EDDAHAHAHAHAG-NH_2 complexes involve a carboxylic oxygen of the acidic terminus EDD-, and this can be the difference which makes more stable the Zn(II) complexes of the latter. At alkaline pH, the two systems become equivalent, since coordination modes for L2 and Ac-EDDAHAHAHAHAG-NH_2 ($3N_{Im}$; HO^-) are the same.

In Figures S37 and S38 (ESI†), the competition diagrams involving L1 and Ac-EDDHAHAHAHAHG-NH_2 complexes are plotted: both of them have five His residues alternated with other amino acids. As in the previous case, the alanine-substituted peptide is a less effective Cu(II) ligand than L1 where histidines are alternated with a glutamic acid, a glycine and two serines. The explanation of this behaviour can be the same as above, although, here both the ligands contain carboxylate side chains which, in principle, can be involved in coordination. For Zn(II) complexes, up to pH 6 (where precipitation occurs in the Zn(II)/L1 system), the difference in stability between the two systems is very small.

A comparison between alternate and consecutive His sequence is shown in Fig. S39 (ESI†), where the competition plot between L1 and the peptide Ac-THHHHYHGG-NH_2 to form Cu(II) complexes is reported. Both the ligands contain 5 histidines, but the alternate sequence seems to be more effective in binding the Cu(II) ion at physiological pH, in agreement with literature where it is reported that the alternate His-tag -AHAHAHAH- confers more stability to the Cu(II) complexes than the consecutive His-tag with four histidines.[27]

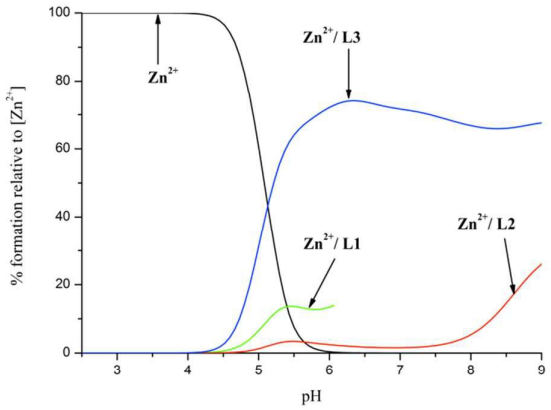

Figure 7 Competition plot for a quaternary solution containing equimolar concentrations (1 mM) of Zn(II), L1, L2 and L3.

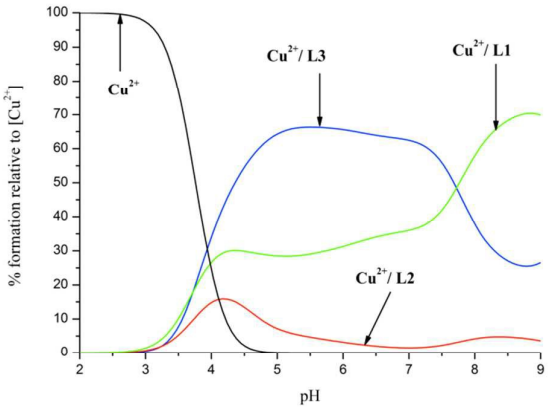

Figure 8 Competition plot for a quaternary solution containing equimolar concentrations (1 mM) of Cu(II), L1, L2 and L3.

Experimental

Materials

All peptides (Ac-FHEHGHSHSHGSGGGGGG-NH_2, Ac-SHSHSHSHS-NH_2, Ac-FHEHGHSHSHGSGGGGGGSDHSGDSKSHSHSHSHS-NH_2) were purchased from KareBay Biochem (USA) (certified purity: 98%) and were used as received. $Zn(ClO_4)_2{\cdot}6H_2O$ and $Cu(NO_3)_2{\cdot}3H_2O$ were extra pure products (Sigma-Aldrich); the concentration of their stock solutions were standardised by EDTA titration and periodically checked *via* ICP-MS. The carbonate-free stock solutions of 0.1 mol dm^{-3} KOH and NaOH were purchased from Sigma-Aldrich and then potentiometrically standardized with the primary standard potassium hydrogen phthalate (99.9% purity). All sample solutions were prepared with freshly doubly distilled water. The $HClO_4$ stock solution was prepared by diluting concentrated $HClO_4$ (Sigma-Aldrich) and then standardized with KOH or NaOH. The ionic strength was adjusted to 0.1 mol dm^{-3} by adding $NaClO_4$ (Sigma-Aldrich). Grade A glassware was employed throughout.

Potentiometric measurements

View Article Online
DOI: 10.1039/C8NJ00533H

Stability constants for proton and metal complexes were calculated from pH-metric titration curves registered at *T*=298 K and ionic strength 0.1 mol dm^{-3} ($NaClO_4$); experimental details are reported as Supplementary Information (Tables S7 and S8, ESI†). The potentiometric apparatus consisted of a Metrohm 905 Titrando pH-meter system provided with a Mettler-Toledo InLab® Micro, glass-body, micro combination pH electrode and a dosing system 800 Dosino, equipped with a 2 ml micro burette. High purity grade argon was gently blown over the test solution in order to maintain an inert atmosphere. A constant-speed magnetic stirring was applied throughout. Solutions were titrated with 0.1 mol dm^{-3} carbonate-free KOH or NaOH. The electrode was daily calibrated for hydrogen ion concentration by titrating $HClO_4$ with alkaline solution under the same experimental conditions as above. The standard potential and the slope of the electrode couple were computed by means of Glee[35] program. The purities and the exact concentrations of the ligand solutions were determined by the Gran method.[36] The HYPERQUAD[37] program was employed for the overall (β) and step (K) stability constant calculations, referred to the following equilibrium:

$$pM + qL + rH \leftrightarrows M_pL_qH_r$$

(charges omitted; p is 0 in the case of ligand protonation; r can be negative). Reported *K*a values are instead the acid dissociation constants of the corresponding species. The computed standard deviations (referring to random errors only) were given by the program itself and are shown in parentheses as uncertainties on the last significant figure. Hydrolysis constants for Zn(II) and Cu(II) ions were taken from the literature.[21, 38] The distribution diagrams were computed using the HYSS program.[39] The overall metal binding ability can be evaluated in a wide pH range by computing and plotting the competition diagrams, starting from the binary speciation models. A solution containing the metal and the two (or more) ligands (or vice versa) is simulated, admitting that all the components compete with each other to form the respective binary complexes, without mixed species formation. This is a reasonable approximation in the case of peptides, which most often form only 1:1 complexes in which the peptide completely wraps the metal ion.

Mass spectrometric measurements

High-resolution mass spectra were obtained on a Bruker MicrOTOF-Q spectrometer (Bruker Daltonik, Bremen, Germany), equipped with an Apollo II electrospray ionization source with an ion funnel. The mass spectrometer was operated in the positive ion mode. The instrumental parameters were as follows: scan range m/z 300-4000, dry gas-nitrogen, temperature 453 K, and ion energy 5 eV. The capillary voltage was optimized to the highest S/N ratio and it was 4800 V. The small changes in voltage (±500 V) did not significantly affect the optimized spectra. The samples were prepared in a 1:1 acetonitrile-water mixture at different pH values (experimental details are reported in Table S9, ESI†). The samples were infused at a flow rate of 3 µL min^{-1}. The instrument was calibrated externally with a Tunemix™ mixture (Bruker Daltonik, Germany) in quadratic regression mode. Data were processed using the Bruker Compass DataAnalysis 4.0 program. The mass accuracy for the calibration was better than 5 ppm, enabling together with the true isotopic pattern (using SigmaFit) an unambiguous confirmation of the elemental composition of the obtained complex.

Spectroscopic measurements

The absorption spectra were recorded on a Varian Cary50 Bio and Varian Cary300 Bio spectrophotometers, in the range 200-800 nm, using a quartz cuvette with an optical path of 1 cm. Circular dichroism (CD) spectra were recorded on a Jasco J-1500 CD spectrometer in the 200-800 nm range, using a quartz cuvette with an optical path of 1 cm in the visible and near-UV range or with a cuvette with an optical path of 0.01 cm in the wavelength range 180-300. The UV-Vis and CD spectroscopic parameters were calculated from the spectra obtained at the pH values corresponding to the maximum concentration of each particular species, based on distribution diagrams. Electron paramagnetic resonance (EPR) spectra were recorded in liquid nitrogen on a Bruker ELEXSYS E500 CW-EPR spectrometer at X-band frequency (9.5 GHz) and equipped with an ER 036TM NMR teslameter and an E41 FC frequency counter. Ethylene glycol (30%) was used as a cryoprotectant for EPR measurements. The EPR parameters were analyzed by computer simulation of the experimental spectra using WIN-EPR SIMFONIA software, version 1.2 (Bruker). The concentrations of sample solutions used for spectroscopic studies were similar to those employed in the potentiometric experiment (experimental details are reported in Tables S10-S12, ESI†).

Conclusions

In the present work, three peptide fragments corresponding to two possible metal binding sites, located in the C-terminal region of the putative fungal protein C4YJH2, have been investigated for their ability to interact with Zn(II) and Cu(II) ions. All the peptides demonstrated a very good affinity for these metals, in a wide pH range; the competition plots reported in Fig. S40-S42 (ESI†) show that complexes formed with Cu(II) are always more stable that those formed with Zn(II) throughout the explored pH range. As a consequence, the two metal ions should compete *in vivo* for these binding sites, copper being favoured by its higher affinity and zinc instead by its larger concentration.

Both the metal ions showed a preference for the binding site corresponding to peptide L1, although the coordination modes are different. As for Zn(II) complexes, all the investigated peptides bind the metal ion by means of three histidine residues ($3N_{Im}$) and an oxygen (carboxylic O^- or a water molecule), with a tetrahedral coordination geometry. The hypothesized molecular structure for Zn(II)/L2 complexes with ($3N_{Im}$; O) configuration at physiological pH is illustrated in

View Article Online
DOI: 10.1039/C8NJ00533H

Fig. S43 (ESI†), by way of example. Concerning copper, it is supposed that, at acidic pH, the metal coordination sphere mainly involves the imidazole ring of histidine residues, while, at neutral or alkaline pH, the coordination of amide nitrogens of the peptidic backbone prevails. In addition, a role for Ser residues has been also hypothesizes, i.e. that of reinforcing the Cu(II)-amide bonds.

The evolutionarily conserved sequence in C4YJH2 is probably fully involved in the task of Zn(II) acquisition and regulation, which is crucial for the growth and subsistence of the pathogenic species like *Candida albicans.* A better knowledge of the thermodynamics behind biological metal transport processes has been obtained, highlighting both the coordination modes used by Zn(II) to bind the proposed amino-acid sequence of C4YJH2 and the competition with Cu(II). This knowledge can contribute to design and tune new antibiotic strategies against all the fungal pathogens using zinc transporters or zincophores containing these or similar peptide sequences in their metal binding sites.

Conflicts of interest

There are no conflicts to declare.

Acknowledgements

The present research was financially supported by: National Science Centre (nr UMO-2014/13/D/ST5/02868), University of Ferrara (FAR 2016), CIRCMSB (Consorzio Interuniversitario di Ricerca in Chimica dei Metalli nei Sistemi Biologici, Bari, Italy), MIUR (Ministero dell'Istruzione, dell'Università e della Ricerca) projects PRIN2015-2015MP34H3 and PRIN2015-2015T778JW) and Erasmus+ programme of the European Union.

Notes and references

1. T. Kourkoumpetis, D. Manolakaki, G. C. Velmahos, Y. C. Chang, H. B. Alam, M. M. De Moya, E. A. Sailhamer and E. Mylonakis, *Virulence*, 2010, **1**, 359-366.
2. S. Campoy and J. L. Adrio, *Biochem. Pharmacol.*, 2017, **133**, 86-96.
3. A. L. Mavor, S. Thewes and B. Hube, *Curr. Drug Targets*, 2005, **6**, 863-874.
4. M. W. McCarthy and T. J. Walsh, *Expert Rev. Anti-infe.*, 2017, **15**, 577-584.
5. M. A. Pfaller, D. J. Diekema and P. Int Fungal Surveillance, *Clin. Microbiol. Infec.*, 2004, **10**, 11-23.
6. M. Blatzer and J.-P. Latgé, *Curr. Opin. Microbiol.*, 2017, **40**, 152-159.
7. M. I. Hood and E. P. Skaar, *Nat. Rev. Microbiol.*, 2012, **10**, 525.
8. E. R. Ballou and D. Wilson, *Curr. Opin. Microbiol.*, 2016, **32**, 128-134.
9. P. K. Walencik, J. Watly and M. Rowinska-Zyrek, *Curr. Med. Chem.*, 2016, **23**, 3717-3729.
10. C. S. Hwang, G. E. Rhie, J. H. Oh, W. K. Huh, H. S. Yim and S. O. Kang, *Microbiol-Sgm*, 2002, **148**, 3705-3713.
11. I. Yike, *Mycopathologia*, 2011, **171**, 299-323.
12. I. Bremner and P. M. May, in *Zinc in Human Biology*, ed. C. F. Mills, Springer London, London, 1989, pp. 95-108.
13. A. N. Besold, E. M. Culbertson and V. C. Culotta, *J. Biol. Inorg. Chem.*, 2016, **21**, 137-144.
14. S. García-Santamarina and D. J. Thiele, *J. Biol. Chem.*, 2015, **290**, 18945-18953.
15. A. N. Besold, B. A. Gilston, J. N. Radin, C. Ramsoomair, E. M. Culbertson, C. X. Li, B. P. Cormack, W. J. Chazin, T. E. Kehl-Fie and V. C. Culotta, *Infect. Immun.*, 2018, **86**.
16. The_UniProt_Consortium, *Nucleic Ac. Res.*, 2017, **45**, D158-D169.
17. G. Butler, M. D. Rasmussen, M. F. Lin, M. A. S. Santos, S. Sakthikumar, C. A. Munro, E. Rheinbay, M. Grabherr, A. Forche, J. L. Reedy, I. Agrafioti, M. B. Arnaud, S. Bates, A. J. P. Brown, S. Brunke, M. C. Costanzo, D. A. Fitzpatrick, P. W. J. de Groot, D. Harris, L. L. Hoyer, B. Hube, F. M. Klis, C. Kodira, N. Lennard, M. E. Logue, R. Martin, A. M. Neiman, E. Nikolaou, M. A. Quail, J. Quinn, M. C. Santos, F. F. Schmitzberger, G. Sherlock, P. Shah, K. A. T. Silverstein, M. S. Skrzypek, D. Soll, R. Staggs, I. Stansfield, M. P. H. Stumpf, P. E. Sudbery, T. Srikantha, Q. Zeng, J. Berman, M. Berriman, J. Heitman, N. A. R. Gow, M. C. Lorenz, B. W. Birren, M. Kellis and C. A. Cuomo, *Nature*, 2009, **459**, 657.
18. M. S. Skrzypek, J. Binkley, G. Binkley, S. R. Miyasato, M. Simison and G. Sherlock, *Nucl. Ac. Res.*, 2017, **45**, D592-D596.
19. H. Sigel and R. B. Martin, *Chem. Rev.*, 1982, **82**, 385-426.
20. G. Borghesani, F. Pulidori, M. Remelli, R. Purrello and E. Rizzarelli, *J. Chem. Soc.-Dalton Trans.*, 1990, 2095-2100.
21. L. D. Pettit and H. K. J. Powell, *The IUPAC Stability Constants Database*, Royal Society of Chemistry, London, 1992-2000.
22. W. Maret, *J. Inorg. Biochem.*, 2012, **111**, 110-116.
23. D. S. Auld, *Biometals*, 2001, **14**, 271-313.
24. S. F. Sousa, A. B. Lopes, P. A. Fernandes and M. J. Ramos, *Dalton Transactions*, 2009, DOI: 10.1039/b904404c, 7946-7956.
25. I. L. Alberts, K. Nadassy and S. J. Wodak, *Protein Science : A Publication of the Protein Society*, 1998, **7**, 1700-1716.
26. J. Peisach and W. E. Blumberg, *Arch. Biochem. Biophys.*, 1974, **165**, 691-708.
27. D. Brasili, J. Watly, E. Simonovsky, R. Guerrini, N. A. Barbosa, R. Wieczorek, M. Remelli, H. Kozlowski and Y. Miller, *Dalton Trans.*, 2016, **45**, 5629-5639.
28. F. Pontecchiani, E. Simonovsky, R. Wieczorek, N. Barbosa, M. Rowinska-Zyrek, S. Potocki, M. Remelli, Y. Miller and H. Kozlowski, *Dalton Trans.*, 2014, **43**, 16680–16689.
29. J. Watly, E. Simonovsky, N. Barbosa, M. Spodzieja, R. Wieczorek, S. Rodziewicz-Motowidlo, Y. Miller and H. Kozlowski, *Inorg. Chem.*, 2015, **54**, 7692-7702.
30. J. Watly, E. Simonovsky, R. Wieczorek, N. Barbosa, Y. Miller and H. Kozlowski, *Inorg. Chem.*, 2014, **53**, 6675−6683.
31. L. Szyrwiel, E. Jankowska, A. Janicka-Klos, Z. Szewczuk, D. Valensin and H. Kozlowski, *Dalton Trans.*, 2008, 6117-6120.

View Article Online
DOI: 10.1039/C8NJ00533H

32. D. Valensin, L. Szyrwiel, F. Camponeschi, M. Rowinska-Zyrek, E. Molteni, E. Jankowska, A. Szymanska, E. Gaggelli, G. Valensin and H. Kozlowski, *Inorg. Chem.*, 2009, **48**, 9042-9042.
33. M. Remelli, D. Brasili, R. Guerrini, F. Pontecchiani, S. Potocki, M. Rowinska-Zyrek, J. Watly and H. Kozlowski, *Inorg. Chim. Acta*, in press., DOI: https://doi.org/10.1016/j.ica.2017.05.070.
34. D. Witkowska, R. Politano, M. Rowinska-Zyrek, R. Guerrini, M. Remelli and H. Kozlowski, *Chem. – Eur. J.*, 2012, **18**, 11088-11099.
35. P. Gans and B. O'Sullivan, *Talanta*, 2000, **51**, 33-37.
36. G. Gran, *Acta Chem. Scand.*, 1950, **4**, 559-577.
37. P. Gans, A. Sabatini and A. Vacca, *Talanta*, 1996, **43**, 1739-1753.
38. G. Arena, R. Cali, E. Rizzarelli and S. Sammartano, *Therm. Acta*, 1976, **16**, 315-321.
39. L. Alderighi, P. Gans, A. Ienco, D. Peters, A. Sabatini and A. Vacca, *Coord. Chem. Rev.*, 1999, **184**, 311-318.

View Article Online
DOI: 10.1039/C8NJ00533H

Investigation on the metal binding sites of a putative Zn(II) transporter in opportunistic yeast species *Candida albicans*

Denise Bellotti,[a] Dorota Łoboda,[b] Magdalena Rowińska-Żyrek,[b,*] Maurizio Remelli[a,*]

Table of contents entry

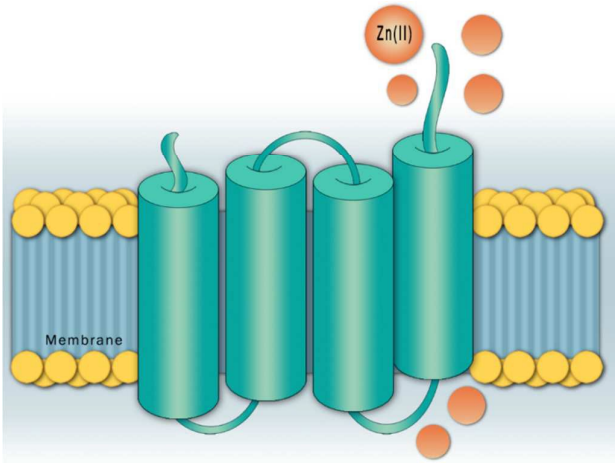

The protein fragment C4YJH2 of *Candida albicans* has the ability to tightly coordinate Zn(II) at its C-terminal region by means of an evolutionarily well-conserved histidine-rich sequence